Broadband nonlinear vibrational spectroscopy by shaping a coherent fiber supercontinuum

Yuan Liu,[1] Matthew D. King, Haohua Tu, Youbo Zhao, and Stephen A. Boppart[1,2,3,*]

[1]*Department of Bioengineering,*
[2]*Department of Electrical and Computer Engineering,*
[3]*Department of Internal Medicine, Beckman Institute for Advanced Science and Technology, University of Illinois at Urbana-Champaign, Urbana, IL 61801, USA*
[*]*boppart@illinois.edu*

Abstract: Vibrational spectroscopy has been widely applied in different fields due to its label-free chemical-sensing capability. Coherent anti-Stokes Raman scattering (CARS) provides stronger signal and faster acquisition than spontaneous Raman scattering, making it especially suitable for molecular imaging. Coherently-controlled single-beam CARS simplifies the conventional multi-beam setup, but the vibrational bandwidth and non-trivial spectrum retrieval have been limiting factors. In this work, a coherent supercontinuum generated in an all-normal-dispersion nonlinear fiber is phase-shaped within a narrow bandwidth for broadband vibrational spectroscopy. The Raman spectra can be directly retrieved from the CARS measurements, covering the fingerprint regime up to 1750 cm^{-1}. The retrieved spectra of several chemical species agree with their spontaneous Raman data. The compact fiber supercontinuum source offers broad vibrational bandwidth with high stability and sufficient power, showing the potential for spectroscopic imaging in a wide range of applications.

OCIS codes: (190.4370) Nonlinear optics, fibers; (300.6230) Spectroscopy, coherent anti-Stokes Raman scattering; (320.6629) Supercontinuum generation; (320.5540) Pulse shaping.

References and links

1. C. L. Evans and X. S. Xie, "Coherent anti-Stokes Raman scattering microscopy: chemical imaging for biology and medicine," Annu. Rev. Anal. Chem. **1**(1), 883–909 (2008).
2. J. P. R. Day, K. F. Domke, G. Rago, H. Kano, H. O. Hamaguchi, E. M. Vartiainen, and M. Bonn, "Quantitative coherent anti-Stokes Raman scattering (CARS) microscopy," J. Phys. Chem. B **115**(24), 7713–7725 (2011).
3. D. L. Marks and S. A. Boppart, "Nonlinear interferometric vibrational imaging," Phys. Rev. Lett. **92**(12), 123905 (2004).
4. T. Hellerer, A. M. K. Enejder, and A. Zumbusch, "Spectral focusing: high spectral resolution spectroscopy with broad-bandwidth laser pulses," Appl. Phys. Lett. **85**(1), 25–27 (2004).
5. C. L. Evans, E. O. Potma, and X. S. Xie, "Coherent anti-Stokes Raman scattering spectral interferometry: determination of the real and imaginary components of nonlinear susceptibility $\chi^{(3)}$ for vibrational microscopy," Opt. Lett. **29**(24), 2923–2925 (2004).
6. J. P. Ogilvie, E. Beaurepaire, A. Alexandrou, and M. Joffre, "Fourier-transform coherent anti-Stokes Raman scattering microscopy," Opt. Lett. **31**(4), 480–482 (2006).
7. H. A. Rinia, M. Bonn, M. Müller, and E. M. Vartiainen, "Quantitative CARS spectroscopy using the Maximum Entropy Method: the main lipid phase transition," ChemPhysChem **8**(2), 279–287 (2007).
8. S. Postma, A. C. W. van Rhijn, J. P. Korterik, P. Gross, J. L. Herek, and H. L. Offerhaus, "Application of spectral phase shaping to high resolution CARS spectroscopy," Opt. Express **16**(11), 7985–7996 (2008).
9. I. Rocha-Mendoza, W. Langbein, P. Watson, and P. Borri, "Differential coherent anti-Stokes Raman scattering microscopy with linearly chirped femtosecond laser pulses," Opt. Lett. **34**(15), 2258–2260 (2009).
10. A. M. Weiner, "Femtosecond pulse shaping using spatial light modulators," Rev. Sci. Instrum. **71**(5), 1929–1960 (2000).
11. Y. Silberberg, "Quantum coherent control for nonlinear spectroscopy and microscopy," Annu. Rev. Phys. Chem. **60**(1), 277–292 (2009).
12. N. Dudovich, D. Oron, and Y. Silberberg, "Single-pulse coherently controlled nonlinear Raman spectroscopy and microscopy," Nature **418**(6897), 512–514 (2002).

#183234 - $15.00 USD Received 15 Jan 2013; revised 8 Mar 2013; accepted 19 Mar 2013; published 28 Mar 2013

13. B. von Vacano, T. Buckup, and M. Motzkus, "Highly sensitive single-beam heterodyne coherent anti-Stokes Raman scattering," Opt. Lett. **31**(16), 2495–2497 (2006).
14. B. von Vacano, W. Wohlleben, and M. Motzkus, "Actively shaped supercontinuum from a photonic crystal fiber for nonlinear coherent microspectroscopy," Opt. Lett. **31**(3), 413–415 (2006).
15. B. von Vacano and M. Motzkus, "Time-resolving molecular vibration for microanalytics: single laser beam nonlinear Raman spectroscopy in simulation and experiment," Phys. Chem. Chem. Phys. **10**(5), 681–691 (2008).
16. K. Isobe, A. Suda, M. Tanaka, H. Hashimoto, F. Kannari, H. Kawano, H. Mizuno, A. Miyawaki, and K. Midorikawa, "Single-pulse coherent anti-Stokes Raman scattering microscopy employing an octave spanning pulse," Opt. Express **17**(14), 11259–11266 (2009).
17. D. Oron, N. Dudovich, and Y. Silberberg, "Single-pulse phase-contrast nonlinear Raman spectroscopy," Phys. Rev. Lett. **89**(27), 273001 (2002).
18. D. Oron, N. Dudovich, and Y. Silberberg, "Femtosecond phase-and-polarization control for background-free coherent anti-Stokes Raman spectroscopy," Phys. Rev. Lett. **90**(21), 213902 (2003).
19. S. H. Lim, A. G. Caster, and S. R. Leone, "Single-pulse phase-control interferometric coherent anti-Stokes Raman scattering spectroscopy," Phys. Rev. A **72**(4), 041803 (2005).
20. S. H. Lim, A. G. Caster, and S. R. Leone, "Fourier transform spectral interferometric coherent anti-Stokes Raman scattering (FTSI-CARS) spectroscopy," Opt. Lett. **32**(10), 1332–1334 (2007).
21. H. Li, D. A. Harris, B. Xu, P. J. Wrzesinski, V. V. Lozovoy, and M. Dantus, "Coherent mode-selective Raman excitation towards standoff detection," Opt. Express **16**(8), 5499–5504 (2008).
22. O. Katz, J. M. Levitt, E. Grinvald, and Y. Silberberg, "Single-beam coherent Raman spectroscopy and microscopy via spectral notch shaping," Opt. Express **18**(22), 22693–22701 (2010).
23. A. Wipfler, J. Rehbinder, T. Buckup, and M. Motzkus, "Full characterization of the third-order nonlinear susceptibility using a single-beam coherent anti-Stokes Raman scattering setup," Opt. Lett. **37**(20), 4239–4241 (2012).
24. H. Kano and H. Hamaguchi, "Ultrabroadband (>2500 cm^{-1}) multiplex coherent anti-Stokes Raman scattering microspectroscopy using a supercontinuum generated from a photonic crystal fiber," Appl. Phys. Lett. **86**(12), 121113 (2005).
25. E. R. Andresen, H. N. Paulsen, V. Birkedal, J. Thøgersen, and S. R. Keiding, "Broadband multiplex coherent anti-Stokes Raman scattering microscopy employing photonic-crystal fibers," J. Opt. Soc. Am. B **22**(9), 1934–1938 (2005).
26. S. Murugkar, C. Brideau, A. Ridsdale, M. Naji, P. K. Stys, and H. Anis, "Coherent anti-Stokes Raman scattering microscopy using photonic crystal fiber with two closely lying zero dispersion wavelengths," Opt. Express **15**(21), 14028–14037 (2007).
27. A. F. Pegoraro, A. Ridsdale, D. J. Moffatt, Y. Jia, J. P. Pezacki, and A. Stolow, "Optimally chirped multimodal CARS microscopy based on a single Ti:sapphire oscillator," Opt. Express **17**(4), 2984–2996 (2009).
28. H. Tu and S. A. Boppart, "Coherent fiber supercontinuum for biophotonics," Laser & Photon Rev, 1–18 (2012).
29. N. Nishizawa and J. Takayanagi, "Octave spanning high-quality supercontinuum generation in all-fiber system," J. Opt. Soc. Am. B **24**(8), 1786–1792 (2007).
30. H. Tu, Y. Liu, J. Lægsgaard, U. Sharma, M. Siegel, D. Kopf, and S. A. Boppart, "Scalar generalized nonlinear Schrödinger equation-quantified continuum generation in an all-normal dispersion photonic crystal fiber for broadband coherent optical sources," Opt. Express **18**(26), 27872–27884 (2010).
31. L. E. Hooper, P. J. Mosley, A. C. Muir, W. J. Wadsworth, and J. C. Knight, "Coherent supercontinuum generation in photonic crystal fiber with all-normal group velocity dispersion," Opt. Express **19**(6), 4902–4907 (2011).
32. H. Tu, Y. Liu, D. Turchinovich, and S. A. Boppart, "Compression of fiber supercontinuum pulses to the Fourier-limit in a high-numerical-aperture focus," Opt. Lett. **36**(12), 2315–2317 (2011).
33. H. Tu, Y. Liu, J. Lægsgaard, D. Turchinovich, M. Siegel, D. Kopf, H. Li, T. Gunaratne, and S. A. Boppart, "Cross-validation of theoretically quantified fiber continuum generation and absolute pulse measurement by MIIPS for a broadband coherently controlled optical source," Appl. Phys. B **106**(2), 379–384 (2012).
34. J. Jakutis-Neto, J. P. Lin, N. U. Wetter, and H. Pask, "Continuous-wave watt-level Nd:YLF/KGW Raman laser operating at near-IR, yellow and lime-green wavelengths," Opt. Express **20**(9), 9841–9850 (2012).
35. H. Tu, Y. Liu, X. Liu, D. Turchinovich, J. Lægsgaard, and S. A. Boppart, "Nonlinear polarization dynamics in a weakly birefringent all-normal dispersion photonic crystal fiber: toward a practical coherent fiber supercontinuum laser," Opt. Express **20**(2), 1113–1128 (2012).
36. Y. Liu, H. Tu, and S. A. Boppart, "Wave-breaking-extended fiber supercontinuum generation for high compression ratio transform-limited pulse compression," Opt. Lett. **37**(12), 2172–2174 (2012).
37. Y. Liu, Y. J. Lee, and M. T. Cicerone, "Broadband CARS spectral phase retrieval using a time-domain Kramers-Kronig transform," Opt. Lett. **34**(9), 1363–1365 (2009).
38. Y. Liu, Y. J. Lee, and M. T. Cicerone, "Fast extraction of resonant vibrational response from CARS spectra with arbitrary nonresonant background," J Raman Spectrosc **40**(7), 726–731 (2009).

1. Introduction

Vibrational spectroscopy is a label-free technique for investigating the chemical content of samples. Compared to spontaneous Raman scattering, coherent anti-Stokes Raman scattering

#183234 - $15.00 USD Received 15 Jan 2013; revised 8 Mar 2013; accepted 19 Mar 2013; published 28 Mar 2013

(CARS) provides coherent signal enhancement, realizing real-time vibrational imaging [1, 2]. In CARS, pump and Stokes fields generate molecular vibration, which is scattered off by a probe field to create a blue-shifted anti-Stokes field. Experimental and computational methods have been developed to retrieve the informative resonant CARS signal and to reject the non-resonant background, especially for spectroscopic applications [3–9]. Among them, pulse shaping enables coherent control of the driving fields and extracting spectral information in a single-beam alignment-insensitive configuration [10, 11]. Several approaches have been proposed to detect molecular vibrational signatures using a single-beam setup, including sinusoidal-phase [12–14], time-resolved pump-probe [15], spectral focusing [16], and narrow-band probe methods [17–23]. Currently, two of the major challenges in single-beam CARS spectroscopy include a limiting vibrational bandwidth that can be attained by the laser sources, and the non-trivial extraction and representation of the Raman spectrum.

Fiber supercontinuum (SC) presents an alternative to solid-state lasers with extended vibrational bandwidth. The use of fiber SC for CARS spectroscopy has been demonstrated in a multi-beam configuration [24–27]. For single-beam methods, a fiber continuum is preferred over a broadband (<20 fs) solid-state laser due to several notable advantages: (1) environmental stability of passive extracavity spectral broadening; (2) the absence of a trade-off between broad bandwidth and stable operation; and (3) intrinsic compatibility with alignment-free fiber-based components. Unfortunately, few known fiber SC sources have sufficient coherence, bandwidth, and power for coherent control [28]. Previous works have shown using a fiber SC for sinusoidal-phase or time-resolved CARS measurements [14, 15]. However, the applicability of a narrow-band probe [17–23] using a fiber SC has not been demonstrated, possibly due to more demanding spectral phase stability and coherence. Recently, fiber SCs with high coherence, stability, and power have been generated by use of all-normal-dispersion fibers [29–33]. This development can be beneficial to high-precision phase shaping applications.

In this study, we demonstrate single-beam vibrational spectroscopy by narrow-band phase shaping of a coherent fiber SC generated in an all-normal-dispersion nonlinear fiber. The pulse shaping strategy and direct vibrational spectrum retrieval are presented. The retrieved spectra of several chemical species agree with their spontaneous Raman data across the fingerprint regime. The performance and advantages of the fiber SC are discussed as well.

2. Experimental methods

The experimental setup is illustrated in Fig. 1. Pulses of 1041 nm, 180 fs (FWHM), and 80 MHz from a compact Yb:KYW laser (femtoTRAIN IC Model-Z, High Q Laser, Austria) were coupled into a nonlinear dispersion-flattened dispersion-decreased all-normal-dispersion (DFDD-ANDi) fiber (NL-1050-NEG-1, NKT Photonics, Denmark). The fiber was pumped at the slow axis with an input power of 600 mW to generate the SC with an output power of 345 mW (~4.3 nJ of pulse energy). Due to weak birefringence of the fiber, a portion of the SC (21%) was depolarized and discarded by a polarizer. The remaining SC was modulated by a pulse shaper (MIIPS Box 640, Biophotonics Solutions Inc.) and then focused by a near-infrared objective (LUMPlanFl/IR 60xW, N.A. = 0.9, Olympus). The spectral phase of the SC at the objective focus was characterized and compensated by the pulse shaper prior to arbitrary pulse shaping [32, 33].

#183234 - $15.00 USD Received 15 Jan 2013; revised 8 Mar 2013; accepted 19 Mar 2013; published 28 Mar 2013

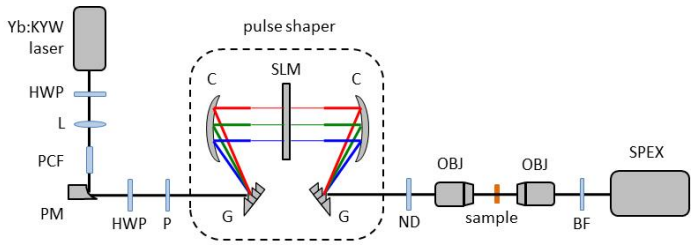

Fig. 1. Schematic of the experimental setup. BF: bandpass filter; C: spherical curved mirror; G: diffraction grating; HWP: half-wave plate; KYW: potassium yttrium tungstate; L: lens; ND: neutral density filter; OBJ: objective; P: polarizer; PCF: photonic crystal fiber; PM: parabolic mirror; SLM: spatial light modulator; Yb: ytterbium; SPEX: spectrometer.

The pulse shaping strategy was simplified from the narrow-band probe approach with impulsive vibrational excitation, as illustrated in Fig. 2 [17, 19, 23]. The SC spectral tail below 900 nm was blocked using a knife-edge at the Fourier plane of the pulse shaper in order to detect CARS signal within this spectral range. A narrow bandwidth centered at the lowest-wavelength peak of the SC spectrum was phase-shifted by ± π/2 radian to serve as the probe pulse. One pixel on the spatial light modulator was modulated, corresponding to a 10 cm^{-1} spectral resolution in the setup. The CARS data of ± π/2 pulses were subsequently acquired for retrieving the Raman spectra.

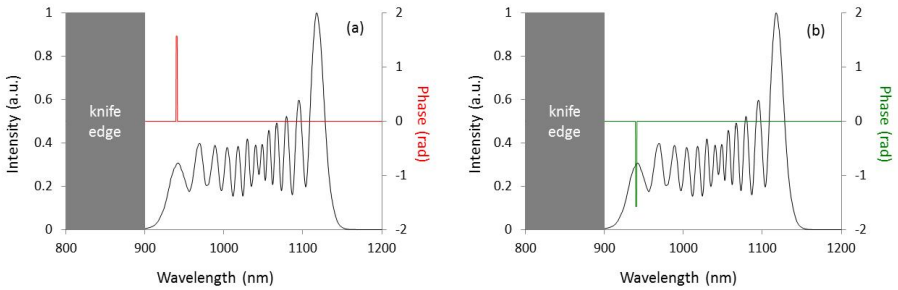

Fig. 2. Pulse shaping strategy for retrieving Raman spectra. The supercontinuum below 900 nm was blocked using a knife-edge at the Fourier plane of the pulse shaper (gray area). The narrow-band probe pulses centered at the shortest-wavelength peak of the supercontinuum spectrum were phase shifted by (a) π/2 (red) or (b) -π/2 (green) radian.

For CARS measurements, the SC power was attenuated by a neutral density filter to 10 mW for solvent samples and to 4 mW for the KGW crystal ($KGd(WO_4)_2$, potassium gadolinium tungstate) at the objective focus. The forward CARS signal from samples between two coverslips was collected by another objective (LUMPlanFl/IR 40xW, N.A. = 0.8, Olympus) and delivered into a spectrometer equipped with an EMCCD camera (ProEM $1600^{(2)}$, Princeton Instruments). The exposure time was 1 ms, and 50 acquisitions were averaged. To validate these spectroscopic measurements, corresponding spontaneous Raman spectra were measured on a commercial confocal Raman microscope (LabRAM HR, Horiba) at the power of 8 mW. The integration time using this Raman microscope was 1 s to achieve the equivalent signal-to-noise ratio.

3. Theoretical modeling

The CARS process can be described in two steps,

$$A(\Omega) = \chi^{(3)}(\Omega)\int_0^\infty E_p(\omega')E_s^*(\omega'-\Omega)d\omega' \qquad (1)$$

#183234 - $15.00 USD Received 15 Jan 2013; revised 8 Mar 2013; accepted 19 Mar 2013; published 28 Mar 2013

$$P(\omega) = \int_0^\infty A(\Omega) E_{pr}(\omega - \Omega) d\Omega \tag{2}$$

Where E_p, E_s, and E_{pr} are the pump, Stokes, and probe fields, respectively. The $\chi^{(3)}(\Omega)$ term is the third-order nonlinear susceptibility, including resonant, $\chi_R^{(3)}(\Omega)$, and non-resonant, $\chi_{NR}^{(3)}$, contributions. For the single-beam approach, the shaped pulses act as E_p, E_s, and E_{pr} simultaneously. The CARS spectra generated by the ± π/2 pulses described earlier are

$$S^{\pm}(\omega) = |P_{NR}(\omega)|^2 + |P_R(\omega)|^2 \mp 2|P_{NR}(\omega)||P_R(\omega)| \mathrm{Im}\{e^{i\phi(\omega)}\} \tag{3}$$

Where ϕ(ω) is the phase induced by the vibrational resonance. The imaginary part of the resonant CARS signal can be obtained by calculating

$$\mathrm{Im}\{P_R(\omega)\} = |P_R(\omega)| \mathrm{Im}\{e^{i\phi(\omega)}\} \sim \frac{S^-(\omega) - S^+(\omega)}{[S^-(\omega) + S^+(\omega)]^{1/2}} \tag{4}$$

The purely resonant term, $|P_R(\omega)|^2$, is relatively small and neglected. A constant prefactor is dropped since it does not affect the spectrum. The Raman spectrum, which is the imaginary part of $\chi_R^{(3)}(\Omega)$, can be retrieved by correcting the impulsive vibrational excitation,

$$\mathrm{Im}\{\chi_R^{(3)}(\Omega)\} = \frac{\mathrm{Im}\{P_R(\Omega)\}}{\int_0^\infty E_p(\omega') E_s^*(\omega' - \Omega) d\omega'} \tag{5}$$

A simulation of this modeling and processing is shown in Fig. 3. The experimental parameters, including the SC spectrum and the pulse shapes, were implemented in the simulation. A hypothetical molecule was assumed to possess vibrations modeled by complex Lorentzians evenly distributed from 600 to 1800 cm^{-1} (Fig. 3(a), blue line). The vibrational excitation spectrum of the compressed SC pulses was calculated to be smooth over the spectral range of interest (Fig. 3(a), gray line). The CARS signal generated by the shaped pulses shows spectral features of $\mathrm{Im}\{\chi_R^{(3)}(\Omega)\}$ on top of the non-resonant CARS spectra, which result from the interference of resonant and non-resonant contributions (Fig. 3(b)). The extracted spectrum recovered the Raman spectrum with only minor distortion (Fig. 3(c)), which originated from the purely resonant contribution neglected in Eq. (3).

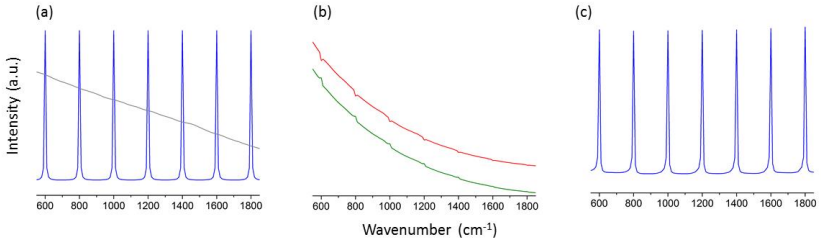

Fig. 3. Theoretical modeling of a retrieved Raman spectrum. (a) Raman spectrum of a hypothetical molecule (blue) and vibrational excitation spectrum of the compressed supercontinuum (gray). (b) The CARS spectra generated by π/2 (red) and -π/2 (green) pulses. Two spectra are offset vertically. (c) The retrieved spectrum which closely resembles the original Raman spectrum.

4. Experimental results

The retrieved and spontaneous Raman spectra of acetone, isopropanol, and toluene are shown in Fig. 4. The CARS spectra agree well with their corresponding Raman data within the fingerprint region. For acetone, the highest detected shift at 1702 cm^{-1} (C = O stretching) is

#183234 - $15.00 USD Received 15 Jan 2013; revised 8 Mar 2013; accepted 19 Mar 2013; published 28 Mar 2013

close to the frequency difference between the two furthest peaks in the SC spectrum (1709 cm^{-1}), which dictates the accessible vibrational bandwidth by the SC. The strong C-C stretching vibration of isopropanol at 819 cm^{-1} is used to estimate the spectral resolution of the system, which is measured to be 13 cm^{-1} (FWHM). At this spectral resolution, the two close peaks of toluene at 1000 cm^{-1} and 1027 cm^{-1} are easily resolved.

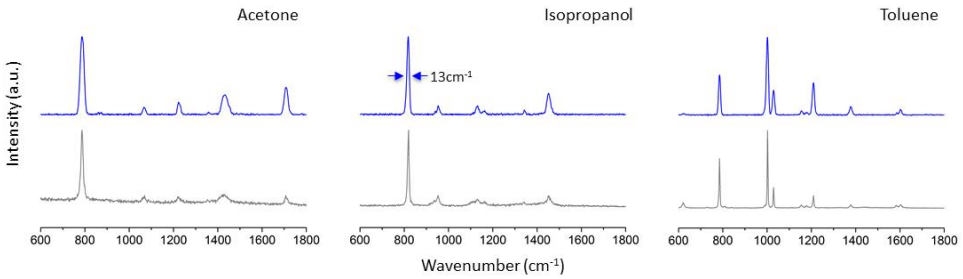

Fig. 4. Retrieved Raman spectra (blue) of acetone, isopropanol, and toluene, and their corresponding spontaneous Raman spectra (gray). The retrieved spectra are vertically offset for comparison. The CARS measurements show good agreement with the spontaneous data. The peak of isopropanol at 819 cm^{-1} is used to quantify the spectral resolution (13 cm^{-1}, FWHM).

The retrieved and spontaneous Raman spectra of a KGW crystal at two orientations ($E||N_g$, $E||N_m$: input electric field parallel to the N_g and N_m refractive index axes, respectively) are shown in Fig. 5. The CARS measurement is sensitive to the orientation of the crystal. In the $E||N_g$ orientation, the CARS data reproduce two major shifts at 767 cm^{-1} and 900 cm^{-1} as in the Raman spectrum [34]. In the $E||N_m$ orientation, the peak at 767 cm^{-1} is observed to be much weaker in both the retrieved and Raman spectra.

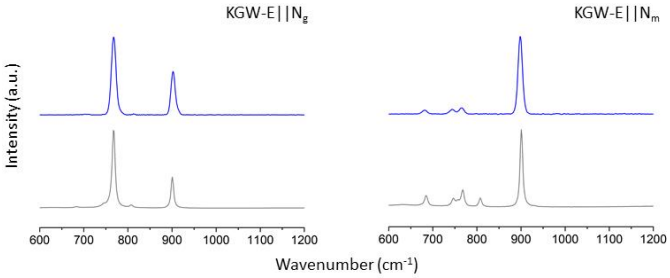

Fig. 5. Retrieved Raman spectra (blue) of a KGW crystal at two orientations ($E||N_g$, $E||N_m$) and their corresponding spontaneous Raman spectra (gray). The retrieved spectra are vertically offset for comparison. The CARS measurements reproduce the orientation-sensitive spontaneous Raman spectra.

5. Discussion

The spectral broadening of the SC generated in the DFDD-ANDi fiber is mainly governed by self-phase modulation, as is evident from its fringe-shaped spectrum. The reduced dispersion and definite spectral phase can be easily compensated to higher orders by a pulse shaper at the focus of a high-NA objective and therefore suitable for coherent control applications. The fiber was pumped at the slow axis to reduce the coupling between the slow and the fast axes, which can degrade the SC generation. An input power of 600 mW was used to induce sufficient spectral broadening for CARS spectroscopy in fingerprint regime. However, a higher input power up to 800 mW has been tested with broader spectrum without damaging the fiber. The depolarization was observed to be higher (21%) than that reported in our previous study (7%) because of a different strand of fiber used [35]. The power, the spectrum and the spectral phase of the SC were measured to be consistent for more than 100 hours of

#183234 - $15.00 USD Received 15 Jan 2013; revised 8 Mar 2013; accepted 19 Mar 2013; published 28 Mar 2013

operation, showing good long-term stability. For more details regarding the coherent fiber SC, including power dependence, phase characterization, and depolarization effects, readers are referred to [30, 32, 33, 35].

The fringe-shaped spectrum might appear to be unsuitable for single-beam CARS spectroscopy because the vibrational excitation can also be structured. Our simulation demonstrates smooth vibrational excitation, and the experiments retrieve Raman spectra across the fingerprint region with good agreement to their corresponding spontaneous Raman data. The detectable spectral range up to about 1750 cm^{-1} is limited by the SC bandwidth, which can be further extended by inducing wave-breaking [36]. The full power of the SC is 345 mW at the fiber output. The nJ-order pulse energy is comparable to some lasers used in single-beam CARS. The SC generation setup is simple and low cost, mainly consisting of a compact Yb:KYW laser and a short piece of nonlinear fiber (9 cm). The broad bandwidth of the fiber SC provides sufficient vibrational excitation for CARS while the moderate pulse energy and compactness can potentially be beneficial for biophotonics applications.

A narrow-band probe pulse shaping strategy was utilized for retrieving Raman spectra, and for determining the molecular contents of samples. The $\pm \pi/2$ phase shifts, as a complex conjugate pair, introduce a small change to the non-resonant background that is used as the local oscillator for homodyne mixing with the resonant signal. Therefore, a signal normalization step that might normally be needed when using 0 and π phase shifts can be relaxed. In addition, the difference spectrum yields the imaginary part of the CARS signal directly without post-processing using the Fourier transform or Kramers-Kronig transformation [19, 20, 37, 38]. Despite the simplicity, this pulse shaping approach has low probe pulse energy and relies heavily on homodyne mixing with the non-resonant signal. The spectra retrieved from the differential measurement can suffer from lower signal-to-noise ratio due to limited dynamic range because the non-resonant signal can easily saturate the detector at low excitation power. By optimizing the detection and pulse shaping scheme, a higher signal-to-noise ratio and faster acquisition could potentially be achieved.

6. Conclusion

Single-beam broadband vibrational spectroscopy has been performed by pulse shaping of a coherent SC generated from a DFDD-ANDi fiber. The SC provides broadband and smooth Raman excitation up to 1750 cm^{-1} with nJ-order pulse energy, enabling its use for single-beam CARS spectroscopy in fingerprint regime. Impulsive excitation with narrow-band probe pulses phase-shifted by $\pm \pi/2$ radian facilitates direct retrieval of Raman spectra. The retrieved spectra of acetone, isopropanol, toluene and a KGW crystal in two orientations agree with their spontaneous Raman measurements. The SC bandwidth can potentially be extended by inducing wave-breaking or by pumping a polarization-maintained DFDD-ANDi fiber. The presented method is promising for spectroscopic imaging of samples in many application areas.

Acknowledgments

We appreciate the collaborative efforts from NKT Photonics, Inc. and Biophotonic Solutions Inc. We thank Prof. Alfred Leitenstorfer for the discussion about collimating the SC. We are grateful for the discussion with Prof. Rohit Bhargava and Dr. Matthew Schulmerich about Raman spectroscopy. We also thank Darold Spillman for his technical support. This work was supported in part by a grant from the National Institutes of Health (NIH R01CA166309, S.A.B.). Additional information can be found at http://biophotonics.illinois.edu.